New evaluation of the CKM-matrix and Unitarity

A. Stocchi

Proceedings of the
VIIIth International Workshop on
Heavy Quarks and Leptons
HQL06

October 2006

Deutsches Museum, Munich

Editors

S. Recksiegel, A. Hoang, S. Paul

This document is part of the proceedings of
HQL06, the full proceedings are available from

http://hql06.physik.tu-muenchen.de

New evaluation of CKM Matrix and Unitarity Triangle parameters

Achille Stocchi
Laboratoire de l'Accélérateur Linéaire,
IN2P3-CNRS et Université de Paris-Sud,
Orsay Cedex, France
on behalf of the **UT***fit Coll.* [1]

1   Introduction

The analysis of the Unitarity Triangle (UT) is one of the key places where the flavour sector of the Standard Model (SM) can be tested with great precision, hence it provides a powerful and maybe unique opportunity to look for sizeable effects beyond the SM. In fact, the successes of the B factories - even well beyond the original expectations - and recently of the Tevatron in the B_s^0 sector, have provided the UT analysis with a rich set of measurements, thus allowing for a precise determination of the parameters of the Cabibbo-Kobayashi-Maskawa (CKM) matrix and, more importantly, for non trivial checks of the internal consistency of the SM flavour picture.

In this paper we will start showing the present knowledge of the Unitarity Triangle fit in the Standard Model and we will continue presenting the status of the Unitarity Triangle analysis beyond the Standard Model using a model independent parametrization of the New Physics effects in $|\Delta F| = 2$ processes. For these analyses we make use of the most recent determinations of theoretical and experimental parameters (updated to Summer 2006). The results and the plots presented in this paper can be found at the URL http://www.utfit.org, where they are continuously updated.

2   Unitarity Triangle in the Standard Model

Before the B factories came into play, UT fits were performed by only using measurements of the sides and of the indirect CP violation parameter ϵ_K of neutral Kaon system. The B factories in few years of measurements completely changed the scenario by providing determinations of all the UT angles, in particular the long awaited

---

[1] M. Bona, M. Ciuchini, E. Franco, V. Lubicz, G. Martinelli, F. Parodi, M. Pierini, P. Roudeau, C. Schiavi, L. Silvestrini, V. Sordini, A. Stocchi, V. Vagnoni

β from $b \to c\bar{c}s$ modes, but also - quite unexpectedly since the penguin pollution in the $B^0 \to \pi^+\pi^-$ decay mode became evident - the α angle. Even more surprisingly, the B factories have been able to close the circuit by providing measurements of the γ angle, even if with large errors so far.

Here below we briefly describe the most relevant measurements entering our SM UT fit:

- The rates of charmed and charmless semileptonic B decays which allow to measure the ratio $|V_{ub}| / |V_{cb}|$.

- The mass difference between the light and heavy mass eigenstates of the $B^0 - \overline{B}^0$ system Δm_d.

- The mass difference of the $B_s^0 - \overline{B}_s^0$ system Δm_s, compared to Δm_d, $\Delta m_d/\Delta m_s$.

- The ε_K parameter, which measures CP violation in the neutral kaon system.

- β from $b \to c\bar{c}s$ modes and from $B^0 \to D^0\pi^0$.

- The angle α, that can be obtained from the $B \to \pi\pi$ and $B \to \rho\rho$ decays, assuming the SU(2) flavour symmetry and neglecting the contributions of electroweak penguins. It can also be obtained using a time-dependent analysis of $B \to (\rho\pi)^0$ decays on the Dalitz plane. The combination of the BaBar and Belle results including all the three methods gives already a quite precise measurement; just restricting to the SM solution, we get $\alpha = (92 \pm 7)^\circ$ at 68% probability.

- The angle γ that can be extracted from the tree-level decays $B \to DK$, using the fact that a charged B can decay into a $D^0(\overline{D}^0)K$ final state via a $V_{cb}(V_{ub})$ mediated process. CP violation occurs if the D^0 and the $\overline{D}^0$ decay to the same final state. The same argument can be applied to $B \to D^*K$ and $B \to DK^*$ decays. Three methods have been proposed: the Gronau-London-Wyler method (GLW), which consists in reconstructing the neutral D meson in a CP eigenstate: $B^\pm \to D^0_{CP\pm}K^\pm$, the Atwood-Dunietz-Soni method (ADS), which consists in forcing the $\overline{D}^0$ (D^0) meson, coming from the Cabibbo-suppressed (Cabibbo-allowed) $b \to u$ $(b \to c)$ transition to decay into the Cabibbo-allowed (Cabibbo-suppressed) $K\pi$ final state - thus looking at the interference between two amplitudes of similar size; the Dalitz method, consisting in studying the interference between the $b \to u$ and the $b \to c$ transitions using the Dalitz plot of D mesons reconstructed into three-body final states (such as $D^0 \to K_s\pi^-\pi^+$). The advantage of this last method is that the full sub-resonance structure of the three-body decay is considered, including interferences such as those used for GLW and ADS methods plus additional interferences due to the overlap
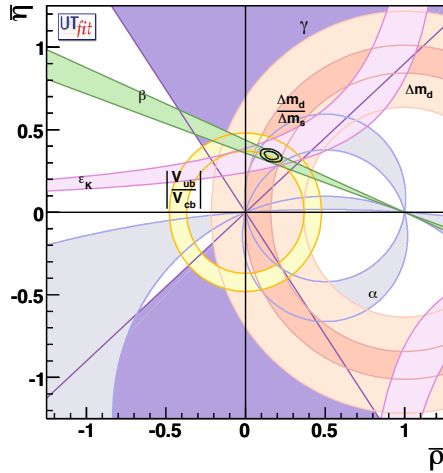
Figure 1: Determination of $\overline{\rho}$ and $\overline{\eta}$ from constraints on $|V_{ub}|/|V_{cb}|$, Δm_d, Δm_s, ε_K, β, γ, and α. 68% and 95% total probability contours are shown, together with 95% probability regions from the individual constraints.

between broad resonances in some regions of the Dalitz plot. The combination of the BaBar and Belle analyses, including all the three methods, yields the two-fold result $\gamma = (82 \pm 19)° \cup (-98 \pm 19)°$ at 68% probability.

For more details on the SM analysis see [1] (for similar work see [2]). In Tab. 1 we summarize the values of the relevant input parameters used in the SM fit, as well as the output of the fit including all the constraints. A graphical view of the fit result in the $(\overline{\rho}, \overline{\eta})$ plane is shown in Fig. 1. From the plot it is clearly visible how impressive the success of the CKM picture is in describing CP violation in the SM: all the various measurements do agree in constraining the apex of the UT at an astonishing level. However, by looking in more detail at Fig. 1, it is interesting to note that the 95% probability regions depicted by the $\sin 2\beta$ and $|V_{ub}|/|V_{cb}|$ constraints, two of the most precise ones used in the fit, show just a bare agreement. In particular, in our analysis we find that while the experimental value of $\sin 2\beta$ is in good agreement with the rest of the fit, the same does not hold for $|V_{ub}|/|V_{cb}|$, which is rather on the high side. It can be shown that this is due to a large value of the inclusive determination of $|V_{ub}|$. Unless this discrepancy should be considered as a hint of NP, it has to be explained by the uncertainties of the theoretical approaches needed to determine $|V_{ub}|$ [3].

Parameter	Value	Gaussian (σ)	Uniform (half-width)
λ	0.2258	0.0014	-
$|V_{cb}|$(excl.)	41.3×10^{-3}	1.0×10^{-3}	1.8×10^{-3}
$|V_{cb}|$(incl.)	41.6×10^{-3}	0.7×10^{-3}	-
$|V_{ub}|$(excl.)	35.0×10^{-4}	4.0×10^{-4}	-
$|V_{ub}|$(incl.)	44.9×10^{-4}	3.3×10^{-4}	-
Δm_d	0.507 ps^{-1}	0.005 ps^{-1}	-
Δm_s	17.77 ps^{-1}	0.12 ps^{-1}	-
$f_{B_s}\sqrt{\hat{B}_{B_s}}$	262 MeV	35 MeV	-
$\xi = \frac{f_{B_s}\sqrt{\hat{B}_{B_s}}}{f_{B_d}\sqrt{\hat{B}_{B_d}}}$	1.23	0.06	-
$\hat{B}_K$	0.79	0.04	0.08
ε_K	2.280×10^{-3}	0.013×10^{-3}	-
f_K	0.160 GeV	fixed	
Δm_K	0.5301×10^{-2} ps^{-1}	fixed	
$\sin 2\beta$	0.675	0.026	-
$\overline{m}_t$	163.8 GeV	3.2 GeV	-
$\overline{m}_b$	4.21 GeV	0.08 GeV	-
$\overline{m}_c$	1.3 GeV	0.1 GeV	-

Parameter	Output	Parameter	Output
$\overline{\rho}$	0.163 ± 0.028	$\overline{\eta}$	0.344 ± 0.016
$\alpha[°]$	92.7 ± 4.2	$\beta[°]$	22.2 ± 0.9
$\gamma[°]$	64.6 ± 4.2	Δm_s [ps^{-1}]	17.77 ± 0.12
$\sin 2\beta$	0.701 ± 0.022	Imλ_t [10^{-5}]	13.8 ± 0.7
$V_{ub}[10^{-3}]$	3.68 ± 0.14	$V_{cb}[10^{-2}]$	4.16 ± 0.06
$V_{td}[10^{-3}]$	8.50 ± 0.27	$|V_{td}/V_{ts}|$	0.208 ± 0.007
R_b	0.381 ± 0.014	R_t	0.904 ± 0.028

Table 1: Top: values of the relevant inputs used in the SM UT fit. The inputs from the α and γ measurements are not shown since we make use of the experimental likelihoods (see text). Bottom: SM UT fit results.
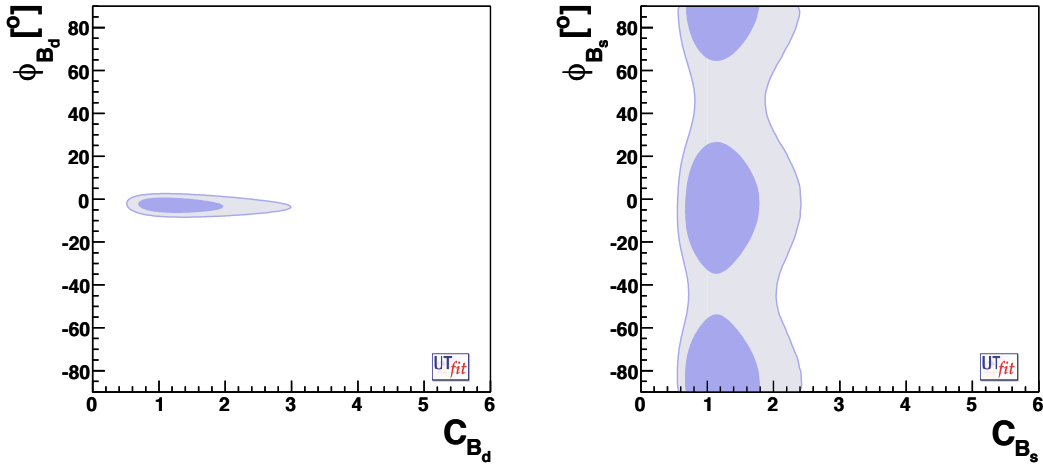
Figure 2: Bounds on the $C_{B_q} - \phi_{B_q}$ planes, from the NP generalized UT fit: 68% and 95% probability regions.

3   New Physics Analysis

Since the mixing processes are described by a single amplitude, they can be parameterized without loss of generality in terms of two parameters quantifying the difference of the amplitude with respect to the SM one. In the case of $B_q^0 - \overline{B}_q^0$ mixing we define

$$C_{B_q}\, e^{2i\phi_{B_q}} = \frac{\langle B_q^0 | H_{\text{eff}}^{\text{full}} | \overline{B}_q^0 \rangle}{\langle B_q^0 | H_{\text{eff}}^{\text{SM}} | \overline{B}_q^0 \rangle}\,, \qquad (q = d, s)$$

where $H_{\text{eff}}^{\text{SM}}$ includes only the SM box diagrams, while $H_{\text{eff}}^{\text{full}}$ includes also the NP contributions. In the absence of NP, we have that $C_{B_q} = 1$ and $\phi_{B_q} = 0$. The experimental quantities determined from the $B_q^0 - \overline{B}_q^0$ mixings are related to their SM counterparts and the NP parameters by the following relations:

$$\Delta m_q^{\text{exp}} = C_{B_q} \Delta m_q^{\text{SM}}\,, \ \ \beta^{\text{exp}} = \beta^{\text{SM}} + \phi_{B_d}\,,$$
$$\alpha^{\text{exp}} = \alpha^{\text{SM}} - \phi_{B_d}\,, \ \ \beta_s^{\text{exp}} = \beta_s^{\text{SM}} - \phi_{B_s}.$$

For the $K^0 - \overline{K}^0$ mixing is instead convenient to introduce a single parameter:

$$C_{\epsilon_K} = \frac{\text{Im}[\langle K^0 | H_{\text{eff}}^{\text{full}} | \overline{K}^0 \rangle]}{\text{Im}[\langle K^0 | H_{\text{eff}}^{\text{SM}} | \overline{K}^0 \rangle]}\,,$$

which implies the following relation for the measured value of ε_K:

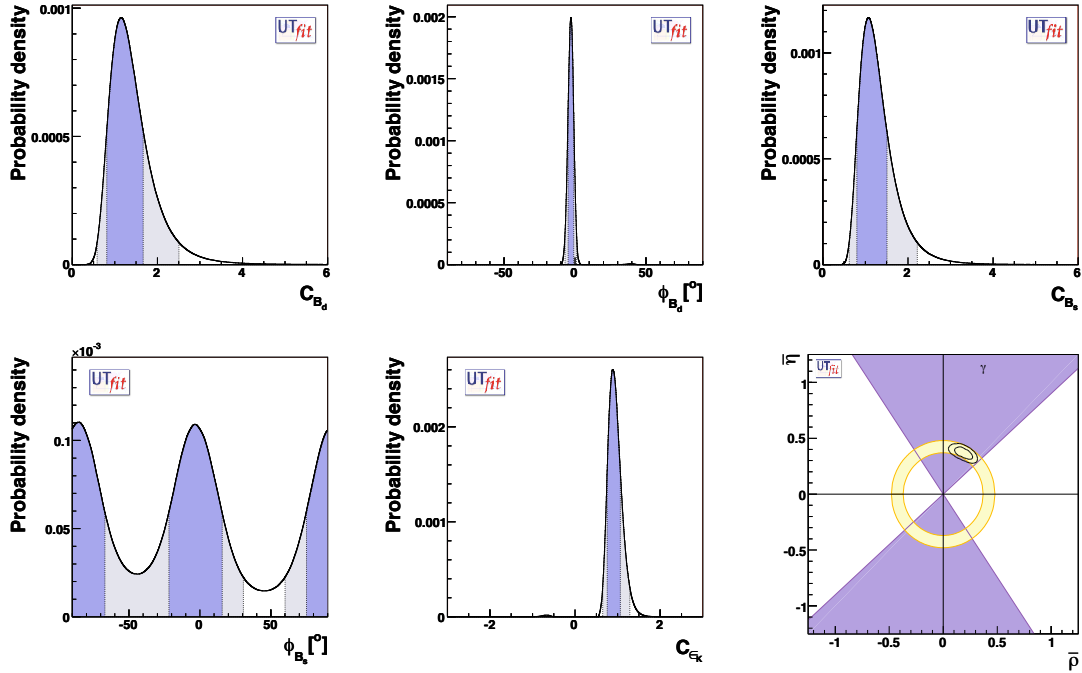$$\varepsilon_K^{\text{exp}} = C_{\epsilon_K}\, \varepsilon_K^{\text{SM}}.$$

5

Figure 3: 1D distributions showing the constraints on ϕ_{B_q}, C_{B_q} and C_{ϵ_K} coming from the NP generalized analysis. The bottom-right plot shows instead the 68% and 95% confidence contours in the $\overline{\rho} - \overline{\eta}$ plane as resulting from the NP generalized fit, superimposed to the 95% confidence regions determined by the $|V_{ub}| / |V_{cb}|$ and γ constraints only.

Δm_K is not considered since the long distance effects are not well under control. With these definitions, NP effects which enter the present analysis are parameterized in terms of 5 real quantities: C_{B_d}, ϕ_{B_d}, C_{B_s}, ϕ_{B_s} and C_{ϵ_K}.

The results of the fit are summarized in Tab. 2. For more details on the NP analysis see [4]. For other recent works on the same subject see [5]. The bounds on the two ϕ_B vs C_B planes are given in Fig. 2. The distributions for C_{B_q}, ϕ_{B_q} and C_{ϵ_K} are shown in Fig. 3, and in the same figure also the fit result in the $\overline{\rho} - \overline{\eta}$ plane is depicted. We see that the *non-standard* solution for the UT with its vertex in the third quadrant, which was present in previous analyses, is now absent thanks to the improved value of $A_{\rm SL}$ by the BaBar Collaboration [6] and to the measurement of $A_{\rm CH}$ by the D0 Collaboration [7]. Furthermore, the measurement of Δm_s strongly constrains C_{B_s}, so that it is already known better than C_{B_d}. Finally, A_{CH} and $\Delta\Gamma_s$ provide the first relevant constraints on ϕ_{B_s}.

Parameter	Output	Parameter	Output	Parameter	Output
C_{B_d}	1.24 ± 0.43	$\phi_{B_d}[^\circ]$	-3.0 ± 2.0	C_{B_s}	1.15 ± 0.36
$\phi_{B_s}[^\circ]$	$(-3 \pm 19) \cup (94 \pm 19)$	C_{ϵ_K}	0.91 ± 0.15		
$\overline{\rho}$	0.87 ± 0.056	$\overline{\eta}$	0.370 ± 0.036	$\alpha[^\circ]$	92 ± 9
$\beta[^\circ]$	24.4 ± 1.8	$\gamma[^\circ]$	63 ± 8	$\mathrm{Im}\lambda_t[10^{-5}]$	14.8 ± 1.4
$V_{ub}[10^{-3}]$	4.00 ± 0.24	$V_{cb}[10^{-2}]$	4.15 ± 0.07	$V_{td}[10^{-3}]$	8.39 ± 0.59
$|V_{td}/V_{ts}|$	0.205 ± 0.015	R_b	0.416 ± 0.026	R_t	0.896 ± 0.061
$\sin 2\beta$	0.752 ± 0.040	$\sin 2\beta_s$	0.039 ± 0.004		

Parameter	Output	Parameter	Output	Parameter	Output
$\overline{\rho}$	0.153 ± 0.030	$\overline{\eta}$	0.347 ± 0.018	$\alpha[^\circ]$	91.3 ± 4.8
$\beta[^\circ]$	22.3 ± 0.9	$\gamma[^\circ]$	66.3 ± 4.8	$\sin 2\beta_s$	0.037 ± 0.002

Table 2: Top: determination of UT and NP parameters from the NP generalized fit. Bottom: determination of UUT parameters from the constraints on α, β, γ, $|V_{ub}/V_{cb}|$, and $\Delta m_d/\Delta m_s$ (UUT fit).

4   Universal Unitarity Triangle

In the context of Minimal Flavour Violation (MFV) extensions of the SM [8,9], it is possible to use the so called Universal Unitarity Triangle (UUT) construction in order to determine the parameters of the CKM matrix independently of NP effects [10]. For this purpose one has to use all the constraints from tree-level processes and from the angle measurements, as well as the $\Delta m_d/\Delta m_s$ ratio, which in MFV scenarios are NP-free. Instead, ϵ_K, Δm_d and Δm_s may receive NP contributions, because of the shifts δS_0^K and δS_0^B of the Inami-Lim functions in the K-$\overline{K}$ and $B_{d,s}$-$\overline{B}_{d,s}$ mixings. With only one Higgs doublet or at small $\tan\beta$ these two contributions are forced to be equal. Instead, for large $\tan\beta$, the two quantities are in general different. In both cases, one can use the output of the UUT given in Tab. 2 and graphically represented in Fig. 4 to constrain $\delta S_0^{K,B}$. We get $\delta S_0 = \delta S_0^K = \delta S_0^B = -0.16 \pm 0.32$ for small $\tan\beta$, while for large $\tan\beta$ we obtain $\delta S_0^B = 0.05 \pm 0.67$ and $\delta S_0^K = -0.18 \pm 0.37$. These bounds can be translated into lower bounds on the MFV scale [11]: $\Lambda > 5.5$ TeV at 95% probability for small $\tan\beta$ and $\Lambda > 5.1$ TeV at 95% probability for large $\tan\beta$.
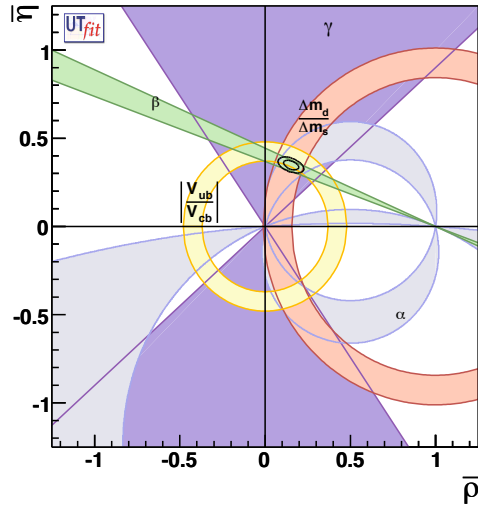
Figure 4: Determination of $\overline{\rho}$ and $\overline{\eta}$ from the constraints on α, β, γ, $|V_{ub}/V_{cb}|$, and $\Delta m_d/\Delta m_s$ (UUT fit).

5   Conclusions

In this paper we have presented updated analyses of the Unitarity Triangle in the Standard Model and beyond, using all the relevant measurements available from the B factories and the Tevatron. Despite the great number of measurements employed in the fit, and the remarkable precision achieved with some of them, the SM is still showing an impressive degree of consistency.

We have performed an analysis with a model-independent approach able to describe general extensions of the SM with loop-mediated contributions to FCNC processes. We have shown how the redundant set of measurements nowadays available allow for a simultaneous determination of the CKM parameters, together with the NP contributions to $|\Delta F| = 2$ processes in the K^0, B^0 and B_s^0 sectors.

Furthermore, we have performed a Universal Unitarity Triangle analysis, showing that it is possible to constrain the UUT parameters with excellent accuracy. In this way, we have been able to put limits on new scale in Minimal Flavour Violation scenarios, in the large and small $\tan\beta$ scenarios, up to about 5-6 TeV.

Bibliography

[1] M. Bona *et al.* [UTfit Collaboration], JHEP **0507**, 028 (2005), [arXiv:hep-ph/0501199]; M. Ciuchini *et al.*, JHEP **0107** (2001) 013 [arXiv:hep-ph/0012308].

[2] J. Charles *et al.*, Eur. Phys. J. C **41** (2005) 1 [hep-ph/0406184]; updates at http://ckmfitter.in2p3.fr/.

[3] M. Bona *et al.* [UTfit Collaboration], [arXiv:hep-ph/0606167].

[4] M. Bona *et al.* [UTfit Collaboration], JHEP **0603**, 080 (2006), [arXiv:hep-ph/0509219];

[5] Z. Ligeti, M. Papucci and G. Perez, Phys. Rev. Lett. **97** (2006) 101801 [arXiv:hep-ph/0604112]; Y. Grossman, Y. Nir and G. Raz, arXiv:hep-ph/0605028; F. J. Botella, G. C. Branco and M. Nebot, arXiv:hep-ph/0608100.

[6] B. Aubert *et al.* [BABAR Collaboration], Phys. Rev. Lett. **96** (2006) 251802 [arXiv:hep-ex/0603053].

[7] D0 Collaboration, D0 Conference note 5189; see also G. Borissov, "D0 results on CP violation phase in B_s system". ICHEP06, Moscow (Russia)

[8] M. Blanke *et al.*, arXiv:hep-ph/0604057.

[9] G. Isidori and P. Paradisi, arXiv:hep-ph/0605012.

[10] A. J. Buras *et al.*, Phys. Lett. B **500**, 161 (2001) [arXiv:hep-ph/0007085].

[11] G. D'Ambrosio *et al.*, Nucl. Phys. B **645**, 155 (2002) [arXiv:hep-ph/0207036].